

Submicron AlGa_N/Ga_N HEMTs With Very High Drain Current Density Grown by Plasma-Assisted MBE on 6H-SiC

Nils G. Weimann, Michael J. Manfra, Subhasish Chakraborty, and Donald M. Tennant

Abstract—High electron mobility transistors (HEMTs) were fabricated from AlGa_N/Ga_N layers grown by plasma-assisted molecular beam epitaxy on semi-insulating 6H-SiC substrates. Room-temperature Hall effect measurements yielded a polarization-induced 2DEG sheet charge of $1.3 \cdot 10^{13} \text{ cm}^{-2}$ and a low-field mobility of $1300 \text{ cm}^2/\text{V}\cdot\text{s}$. Submicron gates were defined with electron beam lithography using an optimized two-layer resist scheme. HEMT devices repeatedly yielded drain current densities up to 1798 mA/mm , and a maximum transconductance of 193 mS/mm . This is the highest drain current density in any AlGa_N/Ga_N HEMT structure delivering significant microwave power reported thus far. Small-signal testing of $50\text{-}\mu\text{m}$ wide devices revealed a current gain cutoff frequency f_T of 52 GHz , and a maximum frequency of oscillation f_{max} of 109 GHz . Output power densities of 5 W/mm at 2 GHz , and 4.9 W/mm at 7 GHz were recorded from $200\text{-}\mu\text{m}$ wide unpassivated HEMTs with a load-pull setup under optimum matching conditions in class A device operation.

Index Terms—Aluminum gallium nitride, gallium nitride, microwave power FETs, MODFETs, molecular beam epitaxy (MBE).

I. INTRODUCTION

AlGa_N/Ga_N HEMTs represent a promising technology platform for microwave high-power solid-state amplifiers. The high breakdown voltage, high electron mobility, high saturation velocity, and the large 2DEG carrier concentration along with the high thermal conductivity of SiC substrates enable AlGa_N/Ga_N high-power microwave HEMTs with theoretical power performance ten times higher than similar GaAs devices. Very high RF power densities have been reported for devices fabricated from MOCVD-grown layers (11 W/mm [1], [2]), as well as devices built on molecular beam epitaxy (MBE)-grown films (8 W/mm [3]) on semi-insulating 4H-SiC substrates. Our group previously reported unpassivated devices grown by plasma-assisted MBE on 6H-SiC substrates with a power density of 6 W/mm at 2 GHz [4]. Device operation beyond S-band requires the realization of submicron gate lengths. We have adapted a manufacturable bilayer resist scheme [5] for AlGa_N/Ga_N HEMT structures resulting in T-gates with a

foot length of 200 nm . In this letter, we report on the device performance of submicron HEMTs from layers grown by plasma-assisted MBE on 6H-SiC substrates.

II. EPITAXIAL STRUCTURE AND HEMT DEVICE TECHNOLOGY

AlGa_N/Ga_N HEMT structures were grown by plasma-assisted MBE directly on 6H-SiC substrates, commercially available from Sterling Semiconductors, Inc. The substrates receive an additional Chemical Mechanical Polishing prior to the MBE growth of the device structure. A 30-nm thick AlN layer serves as a nucleation layer, followed by an undoped Ga_N buffer of $2\text{-}\mu\text{m}$ thickness. The barrier consists of a $300\text{-}\text{\AA}$ thick AlGa_N film with an aluminum mole fraction of approximately 34%. To improve the resistance of the ohmic contacts, the top half of the barrier is doped *n*-type with silicon to a concentration of $8 \cdot 10^{17} \text{ cm}^{-3}$. The structure is capped with a $50\text{-}\text{\AA}$ thick undoped Ga_N film to increase the effective Schottky barrier, which improves the breakdown characteristics and decreases the gate leakage [6]. The entire epilayer is grown at a substrate temperature of $745 \text{ }^\circ\text{C}$. By room temperature Hall measurements, we obtained a sheet carrier concentration of $1.3 \cdot 10^{13} \text{ cm}^{-2}$ along with an electron mobility of $1300 \text{ cm}^2/\text{Vs}$, which corresponds to a sheet resistivity of $370 \text{ }\Omega/\square$.

Ohmic contacts are defined with electron beam lithography using a single layer resist. The Ti 200 \AA /Al 1000 \AA /Ni 550 \AA /Au $450\text{-}\text{\AA}$ ohmic contact stack is alloyed at $850 \text{ }^\circ\text{C}$ in nitrogen atmosphere to yield a transfer resistance of $0.6 \text{ }\Omega\cdot\text{mm}$, as measured by linear TLM. The devices are then mesa-isolated with a shallow chlorine-based ICP etch; the mesa regions are defined with a contact lithography step. The etch depth is limited to 1500 \AA ; no damage to the 2DEG is observed as evidenced by the agreement between sheet resistance measured by Hall on as-grown samples and the sheet resistance derived from the TLM measurement after the mesa isolation etch. The submicron gates are defined with electron beam lithography. We adapted a recently developed bilayer process [5] to T-gate fabrication on AlGa_N/Ga_N HEMT epilayers. The gate lines were exposed in a JEOL model JBX-9300FS electron beam nanolithography system [7] operating at 100-kV . Ni/Au is deposited by electron beam evaporation to produce the gate Schottky contacts. As the final step in the HEMT fabrication, a coplanar test frame is defined with optical contact lithography. A $5000\text{-}\text{\AA}$ thick gold layer is deposited by electron beam evaporation. The HEMT devices are not passivated with Si₃N₄ prior to device testing.

Manuscript received September 27, 2002; revised October 22, 2002. The review of this letter was arranged by Editor D. Ritter.

N. G. Weimann, M. J. Manfra and D. M. Tennant are with Lucent Technologies Bell Laboratories, Murray Hill, NJ 07974 USA (e-mail: weimann@lucent.com).

S. Chakraborty is with Lucent Technologies Bell Laboratories, Murray Hill, NJ 07974 USA, and also with the Department of Physics, Michigan State University, East Lansing, MI 48824 USA.

Digital Object Identifier 10.1109/LED.2002.806298

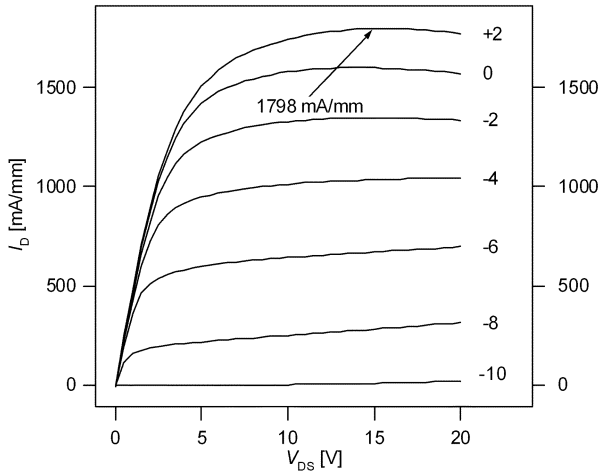


Fig. 1. I - V curve of HEMT with $0.2 \mu\text{m} \times 50 \mu\text{m}$ gate.

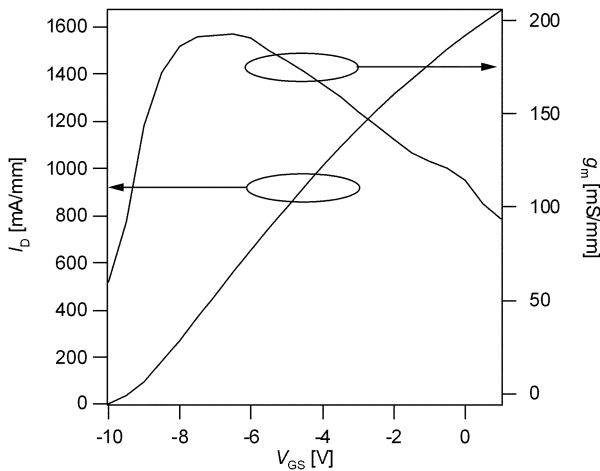


Fig. 2. Drain current and transconductance at $10 V_{DS}$.

III. DEVICE TEST RESULTS AND DISCUSSION

Transconductance and current-voltage (I - V) curves are recorded during the S -parameter measurement of HEMTs with $50\text{-}\mu\text{m}$ periphery using on-wafer coplanar probe tips. The maximum drain current at $+2 V_{GS}$ amounts to 1798 mA/mm (Fig. 1). The transconductance peaks at 193 mS/mm with 10 V applied to the drain. From Fig. 2, the transconductance decreases at higher gate biases, but does not fall below 120 mS/mm up to $0 V_{GS}$. Three-terminal breakdown occurs at $75 V_{DG}$.

Small-signal S -parameters are measured up to 110 GHz with a Hewlett-Packard HP8510XF setup at $10 V_{DS}$. The current gain cutoff frequency f_T and the maximum frequency of oscillation f_{max} are derived by fitting lines with a slope of -20 dB per decade to the small-signal current gain h_{21} and Mason's unilateral gain, respectively. Our best device has intrinsic $f_t = 52 \text{ GHz}$ and $f_{max} = 109 \text{ GHz}$ at $10 V_{DS}$ and $-9 V_{GS}$, close to channel pinchoff (Fig. 3). The intrinsic f_t of our device is comparable to published results (see, for example, [8]). The cutoff frequencies are limited by the relatively thick barrier of 350 \AA , and we expect further increase in the frequency response with thinner barriers.

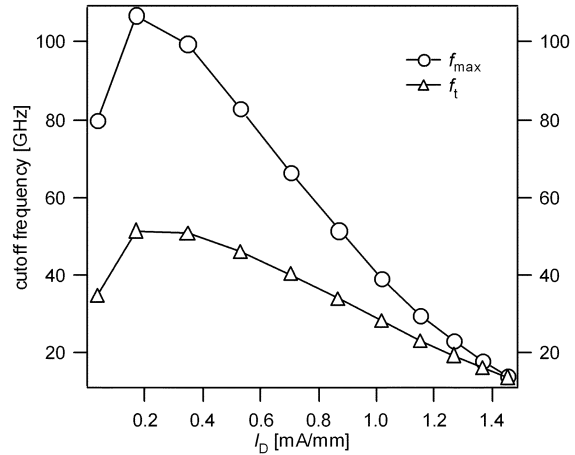


Fig. 3. Small-signal intrinsic cutoff frequencies versus drain current for $0.2 \mu\text{m} \times 50 \mu\text{m}$ HEMT at $10 V_{DS}$.

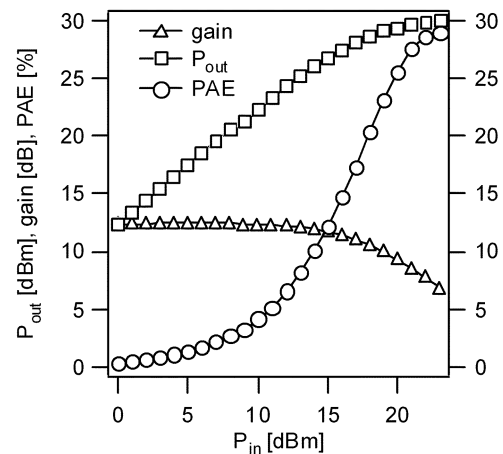


Fig. 4. Load-pull data at 7 GHz for $0.2 \mu\text{m} \times 200 \mu\text{m}$ HEMT at $25 V_{DS}$ and $-5 V_{GS}$.

To evaluate the power performance of our devices, we measured large-signal data using an automated ATN LP1 load-pull setup at 2 and 7 GHz on HEMTs with $0.2\text{-}\mu\text{m}$ long and $200\text{-}\mu\text{m}$ wide gates. At 2 GHz , a saturated output power of 5 W/mm was recorded in class A operation. The measured data at 7 GHz are shown in Fig. 4. The device was biased in class A operation, with 25 volts applied at the drain, and -5 V at the gate. In the small signal regime, we measured a gain of 12 dB . The relatively thick barrier limits the dc transconductance, as well as the RF small-signal gain. We expect to further increase the gain with device structures having thinner barriers. Toward higher input power, the -1 dB compression point is reached at $P_{out} = 27.4 \text{ dBm}$, corresponding to 2.8 W/mm . At the -3-dB compression point, we measured an output power of 29.2 dBm , or 4.3 W/mm . A saturated output power of 29.9 dBm is recorded, equaling a power density of 4.9 W/mm , along with a power added efficiency of 29% . It is noteworthy that a gain of 6.9 dB is still available at the saturation point. We emphasize that all power data were taken without a SiN_x surface passivation layer. The origin of the drain dispersion in AlGaIn-GaN HEMTs is still a subject of intense study. Traps associated with the free surface between gate and drain, the AlGaIn barrier, the GaN buffer,

or the semi-insulating substrate may contribute to drain current dispersion. In the case of our HEMTs grown by plasma-assisted MBE, we measure considerable output power even without surface passivation, suggesting that the free surface plays a less significant role in our layers. The use of passivation layers is currently under investigation in our laboratory. In accord with findings on MOCVD-grown layers [1], [2], we expect further improvements of the output power density with passivation.

IV. SUMMARY AND CONCLUSION

We have fabricated submicron AlGa_N/Ga_N HEMTs from films grown by plasma-assisted MBE directly on semi-insulating 6H-SiC wafers. With a gate length of 0.2 μm , we measured very high drain current densities up to 1.8 A/mm. This is the highest drain current density of any AlGa_N/Ga_N HEMT structure capable of delivering significant microwave power thus far. Intrinsic f_t and f_{max} of these devices were 52 and 109 GHz, respectively. Load-pull measurements at 7 GHz on unpassivated HEMTs yielded a saturated power density of 4.9 W/mm. Power density levels of 4.3 and 2.8 W/mm were recorded for the -3 dB and the -1 -dB compression points, with associated gains of 9 and 11 dB.

REFERENCES

- [1] J. R. Shealy, V. Kaper, V. Tilak, T. Prunty, J. A. Smart, B. Green, and L. F. Eastman, "An AlGa_N/Ga_N high-electron-mobility transistor with an AlN sub-buffer layer," *J. Phys.: Condensed Matter*, vol. 14, pp. 3499–3509, 2002.
- [2] H. Xing, S. Keller, Y. F. Wu, L. McCarthy, I. P. Smorchkova, D. Buttari, R. Coffie, D. S. Green, G. Parish, S. Heikman, L. Shen, N. Zhang, J. J. Xu, B. P. Keller, S. P. DenBaars, and U. K. Mishra, "Gallium nitride based transistors," *J. Phys.: Condensed Matter*, vol. 13, pp. 7139–7157, 2001.
- [3] M. Micovic, J. S. Moon, T. Hussain, P. Hashimoto, W. S. Wong, and L. McCray, "Ga_N HFET's on SiC substrates grown by nitrogen plasma MBE," *Phys. Stat. Sol. A*, vol. 188, pp. 31–35, 2001.
- [4] N. G. Weimann and M. J. Manfra, "AlGa_N/Ga_N HEMT's grown by plasma-assisted MBE on sapphire, HVPE Ga_N, and 6H-SiC," in *29th Int. Symp. on Compound Semiconductors*, Lausanne, Switzerland, 2002.
- [5] L. E. Ocola, D. M. Tennant, and P. D. Ye, "Bilayer process for T-gates and Gamma-gates using 100 kV e-beam lithography," in *Int. Conf. on Micro- and Nano-Engineering*, Lugano, Switzerland, 2002.
- [6] E. T. Yu, X. Z. Dang, L. S. Yu, D. Qiao, P. M. Asbeck, S. S. Lau, G. J. Sullivan, K. S. Boutros, and J. M. Redwing, "Schottky barrier engineering in III-V nitrides via the piezoelectric effect," *Appl. Phys. Lett.*, vol. 73, pp. 1880–1882, 1998.
- [7] D. M. Tennant, R. Fullowan, H. Takemura, M. Isobe, and Y. Nakagawa, "Evaluation of a 100 kV thermal field emission electron-beam nanolithography system," *J. Vac. Sci. Technol. B*, vol. 18, pp. 3089–3094, 2000.
- [8] L. F. Eastman, V. Tilak, J. Smart, B. M. Green, E. M. Chumbes, R. Dimitrov, H. Kim, O. S. Ambacher, N. Weimann, T. Prunty, M. Murphy, W. J. Schaff, and J. R. Shealy, "Undoped AlGa_N/Ga_N HEMT's for microwave power amplification," *IEEE Trans. Electron Devices*, vol. 48, pp. 479–485, 2001.